JOURNAL OF SOLID STATE CHEMISTRY 31, 153–169 (1980)

A Novel Case of Magnetic Relaxation in the ^{99}Ru Mössbauer Spectrum of Na_3RuO_4

TERENCE C. GIBB, ROBERT GREATREX, AND NORMAN N. GREENWOOD

Department of Inorganic and Structural Chemistry, The University of Leeds, Leeds LS2 9JT, England

Received October 10, 1978; in final form March 5, 1979

The magnetic properties of Na_3RuO_4 have been studied using ^{99}Ru Mössbauer spectroscopy. Magnetic hyperfine splitting is seen at temperatures below 30°K. The value of the flux density at 4.2°K (58.58 T) is compatible with a saturation field at an $S = \frac{3}{2}$ Ru^V ion, and at intermediate temperatures approximately follows an $S = \frac{3}{2}$ Brillouin function. The published interpretation of magnetic susceptibility data in terms of tetranuclear intracluster antiferromagnetism is shown to be incorrect, and it is concluded that Na_3RuO_4 shows antiferromagnetic three-dimensional long-range order with a Néel temperature of $T_N = 30 \pm 1$°K. Between 25 and 30°K motional narrowing of the spectrum is seen, which is probably due to a slow spin–spin relaxation within the crystal-field levels of the $^4A_{2g}$ ground state of the Ru^V ion. This is the first observation of relaxation effects in a ^{99}Ru spectrum.

Introduction

In a preliminary study of some ternary oxides of ruthenium with sodium, it was found that Na_3RuO_4 gives the largest magnetic hyperfine field so far observed in a ^{99}Ru Mössbauer spectrum (*1*). The magnetic flux density at the ruthenium nucleus was found to be 58.7 T (587 kG) at 4.2° K, compared with the value of 52.9 T at 4.2°K in $Sr_2Fe^{III}Ru^VO_6$, the only other ruthenium(V) oxide phase studied by Mössbauer spectroscopy (*2*).

The existence of such a magnetic field was not anticipated. Na_3RuO_4 is known (*3, 4*) to have the Na_3NbO_4 structure. The monoclinic lattice (space group $C2/m$) is derived from the NaCl structure by a superlattice ordering of the cations. Groups of four fused RuO_6 octahedra occur in which the four Ru atoms are in a planar lozenge-shaped array. Each $[Ru_4O_{16}]^{12-}$ cluster is isolated from other clusters in the same plane by a belt of 10 NaO_6 octahedra (as illustrated in Fig. 1), and from those in other planes by layers containing only NaO_6 octahedra. Clearly such a structure would not normally be expected to provide the magnetic superexchange paths required for long-range ordering except perhaps at very low temperatures. Although the magnetic susceptibility data for Na_3RuO_4 show a maximum with respect to temperature at ca. 30°K, this has been interpreted in terms of a model involving *localized* antiferromagnetic interactions within each cluster (*5*).

Our observation of magnetic hyperfine splitting in the ^{99}Ru spectrum at 4.2°K can be interpreted in one of two ways. Either the material is magnetically ordered (and we shall show in due course that this implies long-range three-dimensional order) or the

0022-4596/80/020153-17$02.00/0

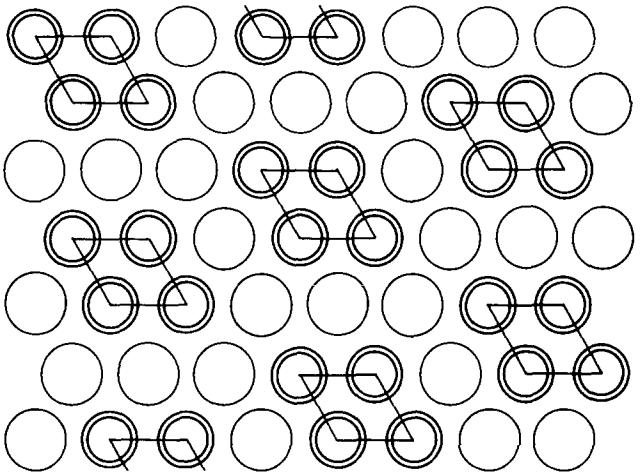

FIG. 1. An idealized representation of a close-packed cation layer in Na_3RuO_4 showing the existence of Ru_4 clusters.

ruthenium(V) spins are paramagnetic but are relaxing very slowly compared with the Mössbauer excited-state lifetime of 2×10^{-8} sec. Slow relaxation has not been recorded previously for ^{99}Ru. In this paper we report a study of the temperature dependence of the Mössbauer spectrum from 4.2 to 30.0°K, which attempts to resolve this interesting problem.

Experimental

The sample of Na_3RuO_4 was kindly supplied by Dr J. Darriet of the University of Bordeaux.

The ^{99}Ru Mössbauer spectra were recorded using a nominal 5-mCi source of ^{99}Rh which had been prepared at AERE, Harwell, by cyclotron bombardment of isotopically enriched ^{99}Ru with ~360 μA·hr of 22 MeV deuterons. The irradiation was followed by chemical separation of the ^{99}Rh activity and coprecipitation with ruthenium metal according to the procedure outlined by Kistner (*6*); finally the source material was annealed at 1000°C under hydrogen. The experimental linewidth of the 90-KeV resonance obtained with this source and an absorber of natural ruthenium metal in the form of a sintered pellet of thickness 140 mg cm^{-2} was 0.26 mm sec^{-1}; this compares well with values recorded previously for similar sources used in this laboratory (0.24–0.36 mm sec^{-1}).

The essential details of the Mössbauer spectrometer have already been described (*1*) except that the NS630 multichannel analyzer was replaced by a MEDA (from Elscint Ltd., Israel).

The powdered sample of Na_3RuO_4 (ca. 1 g) was held between aluminized Mylar disks in a copper mount having an aperture of 1.8 cm^2. The desired temperatures were achieved by use of an Oxford Instruments cryostat, specially designed to allow the source to be maintained at 4.2°K while the absorber temperature was varied. The system incorporated a CLTS cryogenic linear temperature sensor and a DTC-2 precision digital temperature controller capable of maintaining a desired temperature to within ±0.1°K.

The experimental data were analyzed where appropriate using least-squares curve-fitting techniques, and all chemical isomer shifts are quoted relative to an absorber of natural ruthenium metal at 4.2°K.

Results

The Mössbauer spectra of Na_3RuO_4 at 4.2, 10, and 30°K are shown in Fig. 2, and at 20, 25, 27, and 28°K in Fig. 3. At 4.2°K the spectrum shows a well-resolved symmetrical hyperfine pattern which is fully consistent with the 18-line spectrum of a magnetic hyperfine splitting without any significant quadrupole interaction and with a unique value for the magnetic flux density (*7*). The chemical isomer shift is typical of ruthenium (V). The solid line in Fig. 2 is a least-squares fit in which the only variables are the magnetic flux density B, the linewidth Γ, the chemical isomer shift δ, and the usual intensity and baseline scaling parameters. The individual line positions and intensities are constrained to the theoretical values for the hyperfine pattern (*7*), and the parameters deduced are given in Table I. The spectrum is essentially the same as that reported earlier for a different sample (*1*), except that a small resonance from a nonmagnetic impurity in

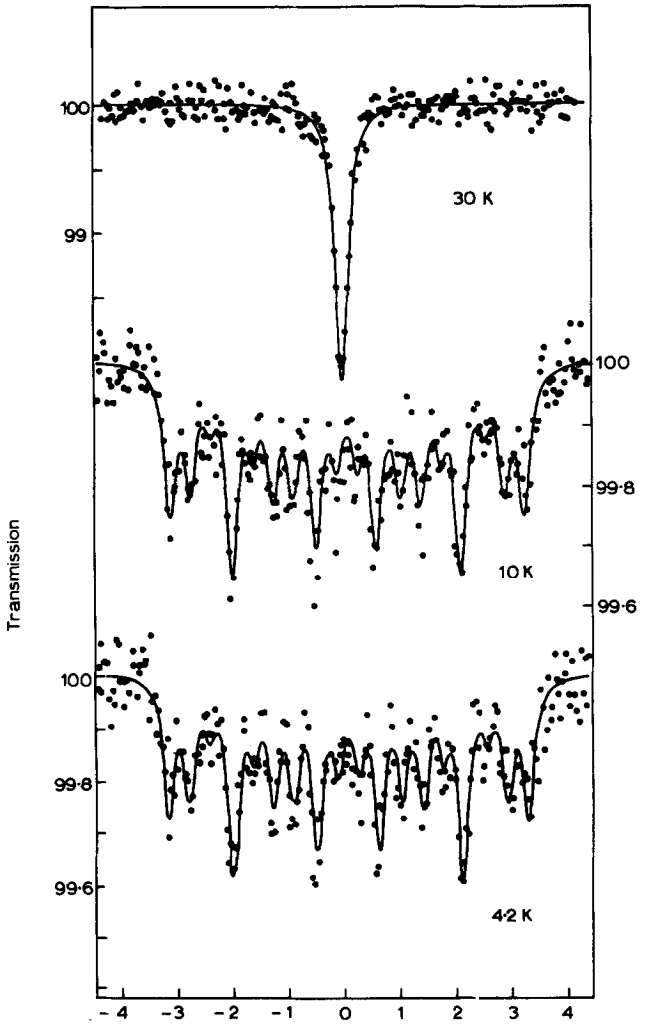

FIG. 2. Mössbauer spectra of Na_3RuO_4 at 4.2, 10, and 30°K.

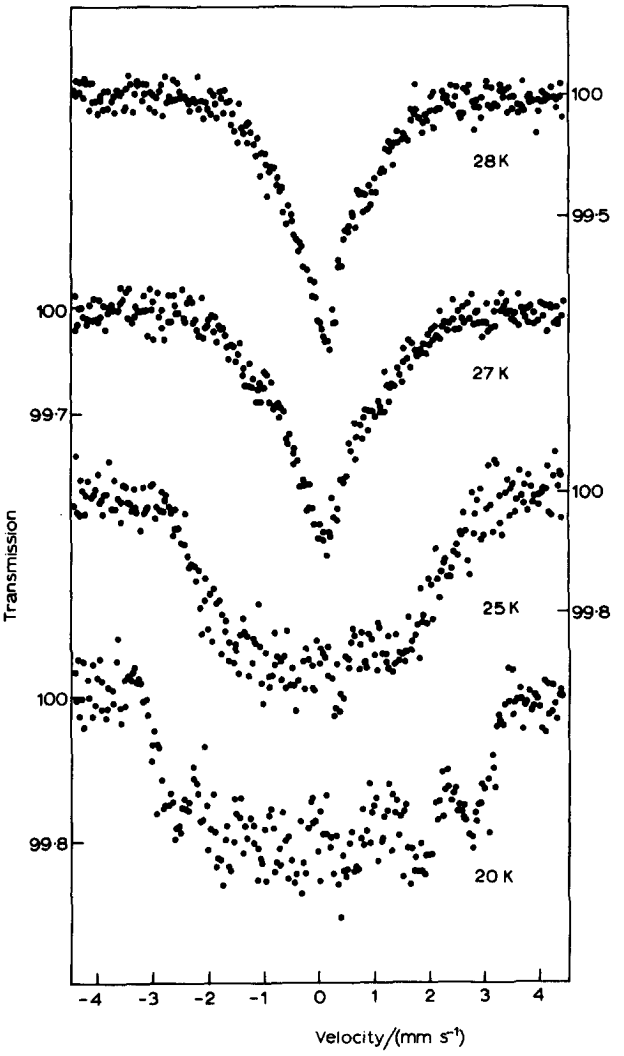

FIG. 3. Mössbauer spectra of Na_3RuO_4 at 20, 25, 27, and 28°K.

TABLE I

^{99}Ru MÖSSBAUER PARAMETERS FOR Na_3RuO_4

Temperature T (°K)	Magnetic flux density B (T)	Linewidth Γ (mm sec^{-1})	Chemical isomer shift δ (mm sec^{-1})	$\chi^2(df)$
4.2	58.58(12)	0.24(1)	0.039(4)	317(239)
10.0	57.90(12)	0.25(1)	0.040(4)	257(239)
30.0	—	0.29(1)	0.053(2)	269(242)

the center of the earlier spectrum is now absent. Accordingly the statistical fit as shown by the χ^2 value is much improved ($\chi^2 = 317$ on 239 degrees of freedom).

The magnetic flux density at the ruthenium nucleus (58.58 ± 0.12 T) is in excellent agreement with that recorded earlier (58.7 T), and is the largest value yet observed for this element in any oxidation state. The only comparable data for the $S = \frac{3}{2}$ ruthenium(V) ion are for the mixed metal perovskite Sr_2FeRuO_6 for which the flux density was found to be 52.9 T at 4.2°K (*2*). Ignoring for the moment the question of the origin of the magnetic field in Na_3RuO_4, but assuming that these values represent the saturation field at $T = 0$°K in each case (the justification for this in Na_3RuO_4 will be made clear shortly), it can be seen that each electron contributes 19.5 and 17.6 T, respectively, to the flux density. These values may be compared with the value of 17.5 T per unpaired electron recorded for the $S = 1$ ruthenium(IV) ion in the perovskite $SrRuO_3$ (*7*). In the case of the two perovskites there is close agreement.

The larger flux density per unpaired electron in Na_3RuO_4 can be explained very effectively by considering covalent overlap. The ground state of $S = \frac{3}{2}$ ruthenium(V) in cubic symmetry is $^4A_2$ and in its behavior is closely analogous to the $^6A_1$ ground state of $S = \frac{5}{2}$ iron(III) in that orbital and dipolar contributions to the flux density are small. In the latter case it has been established (*8*) that increasing covalent overlap causes a reduction in the magnetic flux density of the hyperfine field, as shown, for example, by considering the following compounds (with the coordinations indicated):

FeF_3	$6F^-$	62 T
$NH_4Fe(SO_4)\cdot 12H_2O$	$6H_2O$	~58 T
α-Fe_2O_3	$6O^{2-}$	54 T
$NaFe_3(OH)_6(SO_4)_2$	$4OH^-, 2O^{2-}$	47 T
$FeCl_3$	$6Cl^-$	47 T

It would thus appear that there is substantially less covalent overlap between Ru^V and O^{-II} in Na_3RuO_4 than in Sr_2FeRuO_6. This is also consistent with the increase in chemical isomer shift from 0.039(4) to 0.116(38) mm sec^{-1}; the fractional change in nuclear radius, $\delta R/R$, in ruthenium is opposite in sign to that of iron so that an increase in covalency causes an increase in shift (*8*).

These ideas are also consistent with the available crystal structure data. Sr_2FeRuO_6 is an orthorhombic perovskite (*2*) with cell parameters of $a = 5.53$, $b = 5.56$, and $c = 7.82$ Å; accordingly the Ru–O bond distance (ignoring distortion) will be about 1.96 Å, and not very different from that in $SrRuO_3$. The unit cell of Na_3RuO_4 gives a volume per oxygen of 23.382 Å^3 and corresponds to one octahedral and two tetrahedral (unoccupied) sites (*3*). If these sites were regular as in the true NaCl lattice then the *M*–O bond distance would be about 2.27 Å. Even allowing for the considerable polarizing influence of the Ru^V ion it is not unreasonable to believe that the space requirements of the excess of large Na^+ ions in the lattice help to increase the Ru–O bond distance and reduce the covalent overlap in comparison with Sr_2FeRuO_6.

The computed linewidth of 0.24 ± 0.01 mm sec^{-1} at 4.2°K is consistent with the value of 0.26 mm sec^{-1} for the same source and a ruthenium metal absorber (where the increased absorption cross section should produce some broadening). There is therefore no evidence at this temperature for the slight structural nonequivalence of the ruthenium ions implied by the lozenge shape of the Ru_4 cluster (see Fig. 1).

At 10°K the spectrum is essentially unchanged from that at 4.2°K, except that the magnetic flux density is reduced slightly to 57.90 ± 0.12 T. The linewidth is still narrow at 0.25 ± 0.01 mm sec^{-1}. At 20°K the flux density is decreasing more rapidly, but the spectrum appears broadened, and can

only be fitted with a single magnetic hyperfine pattern is the linewidth is allowed to increase to 0.5 mm sec^{-1}. This trend continues, and at 25°K the computed linewidth is 0.9 mm sec^{-1}. Attempts to fit both of these spectra with the linewidth fixed at 0.24 mm sec^{-1} gave unacceptable results. For whatever reason, the model of a unique hyperfine field is no longer applicable.

At 27 and 28°K the magnetic hyperfine pattern continues to collapse and the spectra consist of broad resonances of compound shape. At 29°K (not shown) the spectrum is a single line with some residual broadening, and at 30°K becomes a sharp line with a width of 0.29 mm sec^{-1}, indicating that the magnetic interactions are no longer affecting the spectrum. As at 4.2°K, there is no discrimination between the two structurally nonequivalent ruthenium sites.

Several possible explanations for these phenomena in Na_3RuO_4 have been investigated in detail, and will now be presented in turn:

(1) The existence of exchange interactions within an isolated tetranuclear cluster;
(2) Long-range magnetic order with a different value of the magnetic flux density for each site;
(3) Long-range magnetic order with isotropic (superparamagnetic) relaxation;
(4) Long-range magnetic order with anisotropic (unspecified) relaxation;
(5) Long-range magnetic order with a crystal-field model for slow spin–spin relaxation;
(6) Paramagnetic relaxation [which for convenience is discussed with (4) and (5)].

In comparing these different possibilities it becomes apparent that the resolution of the hyperfine spectra between 20 and 28°K is unfortunately not as good as one might wish. This is largely due to the distribution across a very broad spectrum of an already low absorption cross section for the ^{99}Ru resonance. However, for a variety of technical reasons it is not possible to obtain any substantial improvement in the data at the present time. Nevertheless, from the discussion which follows it will be seen that a satisfactory description of the magnetism in Na_3RuO_4 does emerge.

(1) *An isolated Cluster Model*

It is significant that the hyperfine splitting disappears at a critical temperature (30°K) which corresponds to the maximum in the magnetic susceptibility (*5*); i.e., as if the compound were antiferromagnetically ordered below a Néel temperature of 30°K. However, the susceptibility data have been interpreted on the basis of strong exchange interactions within the Ru_4 cluster, but negligible exchange interactions between clusters, so that long-range order is absent. Let us consider how this model would influence the Mössbauer spectrum.

The exchange Hamiltonian describing the cluster was taken to be

$$\mathcal{H} = -2J_1(S_1\cdot S_2 + S_2\cdot S_3 + S_3\cdot S_4 + S_4\cdot S_1) - 2J_2 S_2\cdot S_4,$$

where S_i $(i = 1, 2, 3, 4)$ represents the spin operators for the four sites numbered as in Fig. 4, and J_1 and J_2 are the two exchange integrals. Exchange interactions between atoms 1 and 3 and between clusters, and also the crystal-field splitting of the $^4A_2$ configuration, were assumed negligible (*5*). Taking the vector sums

$$S' = S_1 + S_3,$$
$$S'' = S_2 + S_4,$$
$$S = S_1 + S_2 + S_3 + S_4,$$

the eigenstates of the Hamiltonian are given by

$$E(S, S', S'') = -J_1[S(S+1) - S'(S'+1) - S''(S''+1)] - J_2[S''(S''+1) - 15/2].$$

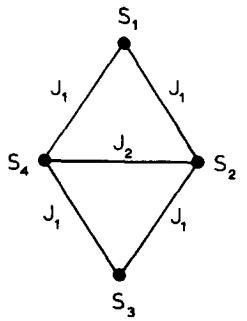

FIG. 4. Schematic diagram of the isolated cluster model.

The susceptibility at a temperature T is then given by using the Van Vleck equation with a Boltzmann population of the eigenstates. Comparison with experimental data yielded $J_1/k = -19.5°K$ and $J_2/k = -22.5°K$ (k is Boltzmann's constant). The three lowest energy states are then $E(0, 3, 3) = 0$, $E(1, 3, 2) = 21$, and $E(1, 3, 3) = 39°K$.

The possible effects upon the Mössbauer spectrum of magnetic exchange between pairs of atoms have been discussed in detail (*9–12*) in connection with the ^{57}Fe resonance in the dimeric complexes Fe[salen Cl]$_2$ and [Fe salen]$_2$O. In these compounds the interaction is between two $S = \frac{5}{2}$ $^6A_1$ Fe^{III} cations, but in other respects the situation is very similar.

Each energy state as characterized by (S, S_z) is derived by taking the appropriate linear combination of the individual (S_i, S_{iz}) states. If only the $S = 0$ ground state is occupied at $T = 0$, then this state cannot show any magnetic interaction (regardless of any question of relaxation time) because the matrix elements of S_{iz} must vanish. Thus in Na_3RuO_4 at 4.2°K, the cluster model as described predicts that 98% of the atoms are in an $S = 0$ nonmagnetic energy state.

The crystal-field splitting will raise the degeneracy of any state for which $S > 0$, and any level for which $S_z \neq 0$ can in principle show a nonzero hyperfine field at the nucleus. However, one has to consider the effects of spin–spin relaxation which will be the dominant ionic relaxation process for this spin configuration. As a fluctuation in the hyperfine field at atom j can only take place by a fluctuation in S_{jz}, this must involve fluctuation between different (S, S_z) states. To conserve angular momentum this can only take place via spin flips involving the (S, S_z) states of *different* clusters, i.e., the relaxation is intercluster rather than intracluster. Because the crystal field splitting is different for each manifold of S, the only spin flips which are energy conserving are those between clusters with the same value of S but with S_z differing by unity. The relaxation thus depends heavily on the thermal population of the S-manifolds, and is sufficiently slow in the ^{57}Fe dimers mentioned to cause line broadening as the temperature is raised (*9–12*).

An example of a ground state with a finite value of S is given by a series of basic iron(III) carboxylates where the magnetic unit is a trimer of $S = \frac{5}{2}$ ions, the ground state being either a fourfold degenerate $S = \frac{1}{2}$ state if the arrangement is an equilateral triangle, or two $S = \frac{1}{2}$ doublets if an isosceles triangle (*13, 14*). The zero-field spectrum at 4.2°K is a sharp quadrupole doublet because relaxation is fast, but the latter can be slowed down by applying a large external magnetic field. The resultant spectrum shows more than one magnetic field because all three spins are not equivalent in the exchange Hamiltonian. It should be noted that for an $S = \frac{1}{2}$ ground state the maximum value of $\langle S_{iz} \rangle$ for three equivalent ions is only $\langle S_{iz} \rangle = \langle S_z \rangle/3$, i.e., the observed field would be only one-fifteenth of the magnetic field normally associated with an $S = \frac{5}{2}$ Fe^{III} ion in an ordered material.

In the present case for an Ru_4 cluster, even if the ground state were an $S = 1$ state, the average observed static hyperfine flux density would correspond to no more than $\langle S_z = \frac{3}{2} \rangle/6$, i.e., only about 10 T. Furthermore, because there are two nonequivalent sites, one might expect to see two distinct

hyperfine fields. A field of the order of magnitude seen experimentally could only be produced by an $S=6$ ferromagnetic cluster, which contradicts the susceptibility data.

We therefore conclude categorically that the model of an exchange interaction within an isolated cluster of four atoms does not provide a correct description of Na_3RuO_4 below 30°K. As we shall now show, the Mössbauer data can be explained only on the basis of long-range magnetic order below 30°K, although it is possible that the intercluster exchange is significantly weaker than the intracluster exchange.

(2) *Multiple Hyperfine Field Model*

The magnetic flux density, $B(T)$, in a long-range ordered antiferromagnetic material has a temperature dependence below the Néel temperature T_N which approximates to the appropriate idealized Brillouin function. Strictly speaking, $B(T)$ is only single valued if all the resonant atoms are on exactly equivalent sites. However, it is not unusual for $^6A_1$ Fe^{III} ions to show the same saturation value of $B(0)$ at sites which differ markedly. This is because $B(0)$ is derived mainly from the Fermi contact term which depends only on the spin S and on covalent overlap, rather than from orbital and dipolar terms which are much more sensitive to the crystal-field symmetry. The $^4A_2$ Ru^V ion is closely analagous, and it is only to be expected that two different sites with six-coordination to oxygen have effectively the same saturation value of $B(T)$.

However, there are numerous examples in the literature of ^{57}Fe spectra where variations in the magnetic characteristics of the nearest-neighbor atoms result in multiple values of $B(T)$ for Fe^{III} ions at temperatures intermediate between 0°K and T_N. A detailed treatment of this effect in mixed oxide systems has been given by Coey and Sawatzky (*15*) using molecular field theory. It was found to give good agreement with experimental data except in the region immediately below the critical temperature where it is often inadequate because of the neglect of time-dependent fluctuations.

An alternative approach by Iyengar and Bhargava (*16, 17*) is to use an *averaged* molecular field, but to include time-dependent fluctuations within the electronic sublevels. This method often gives an excellent representation of data immediately below the critical temperature, and can give a surprisingly good (if perhaps fortuitous) representation at intermediate temperatures where both models can seemingly produce the spectrum broadening observed. However, it is quite clear that for correctness the two methods should be combined to give both a variable molecular field *and* time-dependent fluctuations. The main difficulty is that the magnitude of the numerical calculation is substantially increased thereby, and now includes many more parameters which may not be known accurately.

We have already seen examples of intracluster exchange where magnetic hyperfine splitting is absent. It is also important to note that there is no evidence to suggest that short-range order or even one- or two-dimensional magnetism can produce the static magnetic hyperfine pattern which is seen in Na_3RuO_4 below 20°K. $KFeCl_3$ and $Fe(N_2H_5)_2(SO_4)_2$ both show one-dimensional magnetism (*18,19*), and Rb_2FeF_4 and $RbFeF_4$ both show two-dimensional magnetism (*20,21*); all show a collapse of the ^{57}Fe hyperfine pattern above the critical temperature for three-dimensional ordering. Only a small residual broadening can occur in the temperature range where low-dimensional magnetism occurs. Furthermore, such systems usually show a broad maximum in the susceptibility above the critical temperature for three-dimensional magnetism. This feature is absent in Na_3RuO_4. We can therefore conclude that the magnetism in Na_3RuO_4 is a long-range three-dimensional antiferromagnetic ordering.

In Na_3RuO_4 there are two distinct sites for the Ru^V ion which may differ substantially in their magnetic exchange behavior. Let us assume therefore that each has a different value of $B(T)$ at temperatures above 10°K. The spectra at 20, 25, 27, and 28°K were curve fitted with two superimposed hyperfine patterns of equal intensity with flux densities B_1 and B_2, keeping the linewidth fixed at 0.24 mm sec^{-1}. The final parameters are given in Table II, and the theoretical curves on the same scale as the data in Fig. 3 are shown separately for clarity in Fig. 5. The chemical isomer shifts in these and succeeding calculations had an increased standard deviation, but remained within the range 0.03–0.08 mm sec^{-1}. The fits at 20 and 25°K are quite good as may be seen from the χ^2 values. The change in profile of the outer wings of the spectrum and the accentuation of the central region are faithfully reproduced.

The values of the magnetic flux density are plotted in Fig. 6. The solid curve is the $S=\frac{3}{2}$ Brillouin function calculated for $B(0)=58.6\ T$ and $T_N=30$°K. It can be seen that both B_1 and B_2 have a temperature dependence which is reasonably close to the Brillouin function, and which is not unreasonable for two magnetically nonequivalent $S=\frac{3}{2}$ ions.

However, at 27 and 28°K the agreement is less satisfactory, as may be seen by the large increases in χ^2. The best computed fits are unable to reproduce the comparatively featureless spectra, and in particular cannot give the characteristic sharpness of the central region. Furthermore, the very large differences between B_1 and B_2 seem unreasonble.

It therefore appears that although a multiple hyperfine field model may be adequate from 0 to 25°K, a different explanation, probably involving time-dependent phenomena, may be more appropriate between 25 and 30°K.

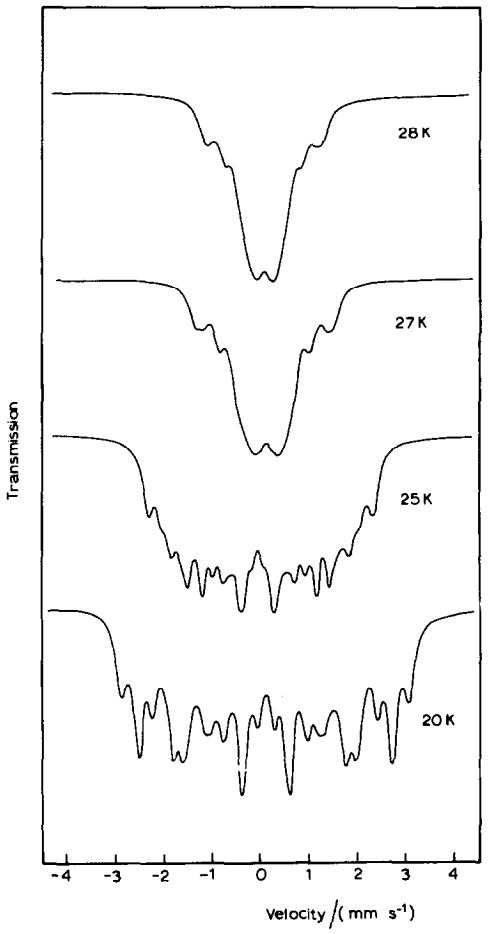

FIG. 5. The least-squares theoretical fits to the data of Fig. 3 from the multiple hyperfine field model (drawn to the identical scale).

TABLE II

PARAMETERS FOR MULTIPLE HYPERFINE FIELD MODEL

Temperature T (°K)	Magnetic flux densities (T) B_1	B_2	$\chi^2(df)$
20.0	53.6(2)	47.6(2)	387(236)
25.0	40.6(3)	32.7(3)	286(231)
27.0	26.2(4)	10.3(2)	567(236)
28.0	22.3(4)	8.0(2)	682(236)

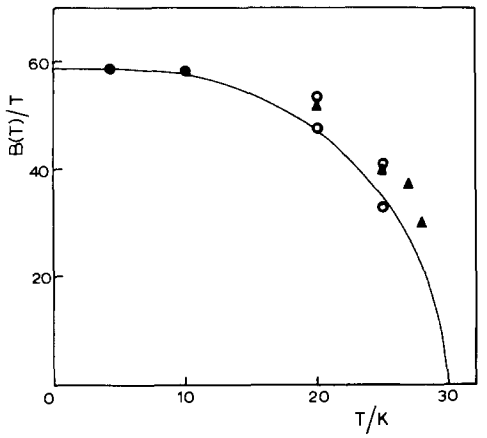

FIG. 6. The magnetic flux density at the ^{99}Ru nucleus as given by the single hyperfine field model (filled circles), multiple field model (open circles), and the isotropic relaxation model (triangles). The solid curve is the $S=\frac{3}{2}$ Brillouin function for $B(0)=58.6$ T and $T_N=30$°K.

(3) *Isotropic (Superparamagnetic) Relaxation Model*

Time-dependent effects have not been recorded previously in the ^{99}Ru hyperfine spectrum, and therefore we have investigated this possibility in detail. Too little is known about Na_3RuO_4 to be able to describe any time-dependent or relaxation effects accurately, and therefore it seemed appropriate to consider in the first instance some simple relaxation models which have the important advantage of being easy to evaluate numerically.

The first of these models (Dattagupta and Blume (*22*)) uses the "strong-collision approximation" to calculate an isotropic relaxation qualitatively similar to, for example, thermal agitation in a superparamagnetic material. The Hamiltonian is assumed to jump at random among a number of states such that the initial and final states are completely uncorrelated. The lineshape is expressed as the real part of

$$I(p)\alpha \sum_L \frac{|M_L|^2+|E_L|^2}{2L+1}\left(\frac{G^\circ_{LL}(p+W)}{1-WG^\circ_{LL}(p+W)}\right)$$

where

$$G^\circ_{LL}(p+W)=\sum_{m_0m_1}\left\{\begin{pmatrix} I_1 & I_0 & L \\ m_1 & -m_0 & M\end{pmatrix}^2 \times/[(p+W)+i\alpha]\right\}.$$

$|M_L|^2$ and $|E_L|^2$ represent the strengths of the magnetic and electric multipoles in the 90-keV radiation, $p=i(\omega-\omega_0)+\Gamma/2$ contains the resonant frequency ω relative to the centroid ω_0 and the linewidth Γ, the coefficient in brackets is the Wigner coefficient coupling the excited (I_1, m_1) and ground (I_0, m_0) states so that the sum extends over all 18 lines in the hyperfine spectrum, W is the jump frequency, $\alpha=(g_0m_0-g_1m_1)\mu_NB$ is the energy difference between states where g_1 and g_0 are the respective g factors, and μ_N is the nuclear magneton.

These expressions were incorporated into an iterative curve-fitting program and used to analyze the data between 20 and 28°K. The parameters of the fits with the linewidth fixed at 0.24 mm sec^{-1} and $|E_2|^2/|M_1|^2=2.72$ (*7*) are given in Table III, and the actual curves shown in Fig. 7 to the same scale as in Fig. 3. If Γ, ω, W, and λ are all in dimensions of mm sec^{-1} then the jump frequency W is converted to a relaxation time τ in seconds by $\tau=1.38\times10^{-8}/W$. The statistical criterion for the goodness of fit, χ^2 is rather better in all cases than for the multiple hyperfine field model, and this is particularly noticeable at 27 and 28°K. This lends considerable support to the suggestion that relaxation behavior is in fact involved. The values of $B(T)$ are included in Fig. 6. The obvious failure of the model is that at 27 and 28°K it gives a broad single-line fit without the structure which obviously exists in the hyperfine data.

It is possible to extend the model by introducing two hyperfine fields and/or two relaxation times, but although a clear improvement is obtained in the statistical fit, we have considerable reservations as to

TABLE III

PARAMETERS FROM THE ISOTROPIC AND ANISOTROPIC RELAXATION MODELS

Temperature T (°K)	Magnetic flux density B (T)	Relaxation time τ ($\times 10^9$/sec)	$\chi^2(df)$
Isotropic			
20.0	51.6(3)	94.3(10.6)	285(239)
25.0	40.0(6)	44.6(5.6)	256(234)
27.0	37.6(5.1)	6.4(1.5)	363(241)
28.0	30.2(4.0)	7.6(1.5)	460(241)
Anisotropic			
20.0	50.7(2)	6.2(7)	391(239)
25.0	39.1(3)	2.2(2)	273(234)
27.0	22.6(6)	3.3(3)	378(241)
28.0	17.9(2)	2.5(2)	468(241)

whether the parameters obtained are meaningful, especially as it is very unlikely that the relaxation in this system is in fact isotropic.

(4) *Anisotropic Relaxation*

In view of the possibility that the relaxation is highly anisotropic, a simple (if physically unrealistic) model was constructed to enable a ready comparison to be made. The calculation was based on results by Blume and Tjon (*23*) for a fluctuating magnetic field directed along the axis of an axially symmetric electric field gradient. Although the latter undoubtedly exists at the resonant site, it does not produce a detectable quadrupole interaction in the ^{99}Ru spectrum. The lineshape is expressed in a similar manner to the isotropic case as the real part of

$$I(p)=\sum_L \frac{|M_L|^2+|E_L|^2}{2L+1} \sum_{m_0 m_1} \times \begin{pmatrix} I_1 & I_0 & L \\ m_1 & -m_0 & M \end{pmatrix}^2 G(p),$$

where

$$G(p)=\sum_{i,j=\pm 1} q_i (j|[p-W-i\alpha F]^{-1}|i).$$

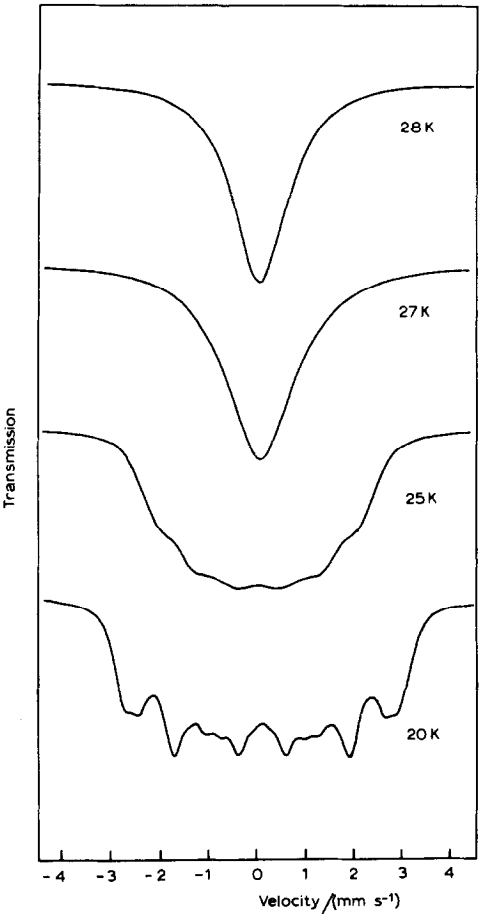

FIG. 7. The least-squares theoretical fits to the data of Fig. 3 from the isotropic relaxation model (drawn to the identical scale).

$\alpha=(g_0 m_0-g_1 m_1)\mu_N B$ as before, F is a matrix for which the elements are the permissable values of $f(t)$ in the Hamiltonian

$$\mathcal{H}=\mathcal{H}_0+g\mu_N B I_z f(t),$$

W is the matrix of transition probabilities between the initial (i) and final (j) electronic states, with the diagonal elements $W_{ii}=-\sum_i W_{ij}(i\neq j)$, and q_i represents the probability of being in the initial state i with $\sum_i q_i=1$.

Let us consider a very naive (and not strictly correct) model in which there are only two states ($i=1,2$) corresponding to the $S_z=$

$+\frac{3}{2}$ and $S_z = -\frac{3}{2}$ states with $f(t) = +1$ and -1, respectively. If the two states exist with equal probability ($q_1 = q_2 = \frac{1}{2}$), i.e., we are considering relaxation in a paramagnetic system, then $W_{12} = W_{21} = W$. The matrix inversion can be carried out explicitly and gives

$$G(p) = (p + 2W)/(p^2 + 2pW + \alpha^2),$$

and evaluation of $I(p)$ is now straightforward. This has been carried out for various values of W and with $B = 58.6$ T, $\Gamma = 0.24$ mm sec^{-1}. Selected spectrum lineshapes are shown in Fig. 8; note that in this case of paramagnetic relaxation the initial inward broadening of the spectrum is not accompanied by an apparent decrease in the maximum magnetic flux density as occurs in relaxation in a magnetically ordered phase. For this reason alone it is possible to completely exclude paramagnetic relaxation as an explanation for the present data.

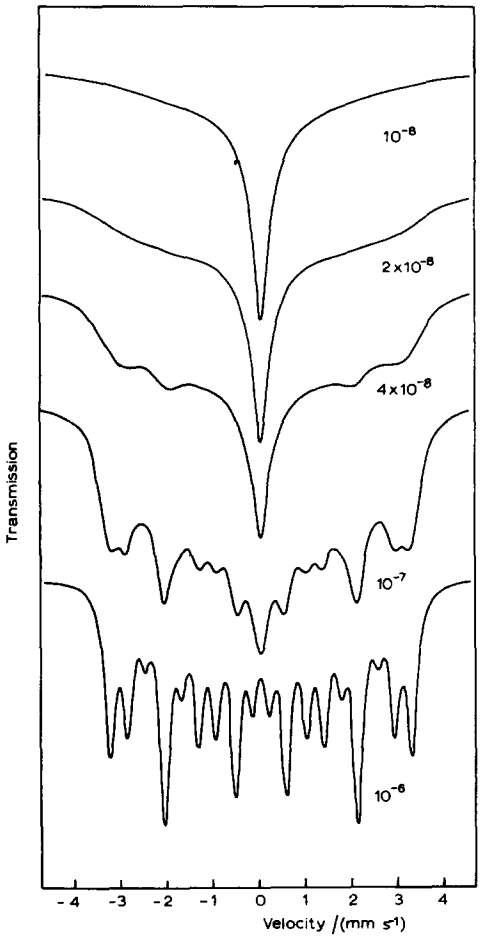

FIG. 8. A simple model for paramagnetic relaxation in ^{99}Ru. The figures are the relaxation times in seconds.

If long-range order is present, then this can be approximated by assuming $W_{12} \neq W_{21}$. At equilibrium $q_1 W_{12} = q_2 W_{21}$. The matrix inversion is more complicated, but can be evaluated to give

$$G(p) = \frac{p + i\alpha(q_1 - q_2) + 2(q_1 W_{21} + q_2 W_{12})}{p^2 + p(W_{12} + W_{21}) + i\alpha(W_{12} - W_{21}) + \alpha^2}.$$

This model was curve fitted to the four spectra between 20 and 28°K using the fractional population $q_1 (= 1 - q_2)$ as a variable and fixing the flux density at 58.6 T and the linewidth at 0.24 mm sec^{-1}. The resultant theoretical curves are shown in Fig. 9 (to the same scale as Fig. 3). An average flux density at the resonant nucleus can then be calculated from $(q_1 - q_2) \times 58.6$ T. Only a single averaged hyperfine field is seen if relaxation is very fast. As the relaxation slows then broadening occurs. The parameters given in Table III are not strictly comparable with those from the isotropic model because the assumptions are different. However, the χ^2 values are roughly comparable, and the flux densities at 20 and 25°K agree well. As expected, the anisotropic relaxation model shows more hyperfine structure in the final fits, but in view of the gross assumptions made in both models their similarity is gratifying and justifies their use in the present instance to simulate time-dependent fluctuations.

(5) *A Crystal-Field Model for Slow Spin–Spin Relaxation*

In view of the good agreement obtained with the two simple relaxation models, it is worth considering whether an appropriate

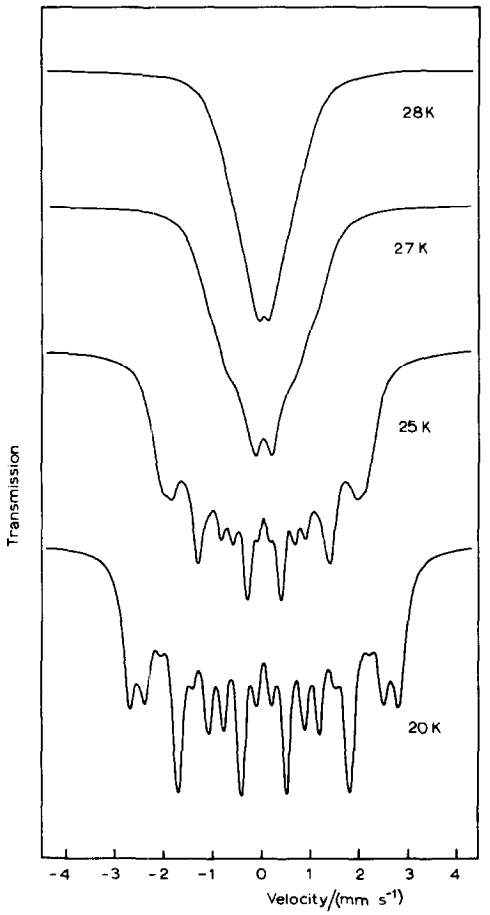

FIG. 9. The least-squares theoretical fits to the data of Fig. 3 from the anisotropic relaxation model (drawn to the identical scale).

mechanism exists for relaxation in Na_3RuO_4, and to see if a more rigorous model for the relaxation can be formulated.

The ^4F free-ion configuration of the $4d^3$ Ru^V ion adopts a fourfold degenerate $^4A_{2g}$ ground state in octahedral symmetry. Under the combined effects of spin–orbit coupling and a trigonal field this splits into two Kramers' doublets corresponding to $S_z = \pm\frac{3}{2}$ and $S_z = \pm\frac{1}{2}$. The separation of these is designated $2D$ with D being negative in sign when the $S_z = \pm\frac{3}{2}$ state lies lowest.

The magnitude of $2D$ in Na_3RuO_4 is unknown, but in view of the large value for the spin–orbit coupling in Ru^V, $\lambda =$ 500 cm^{-1}, it may well be large. The value of $2D$ for Mo^{III} ions ($\lambda \sim 270$ cm^{-1}) substituted into yttrium aluminium garnet is 8–10 cm^{-1} (*24*). Since $2D$ is approximately proportional to λ^2 it would appear that values of $|2D|$ up to at least 30 cm^{-1} are not unreasonable for Ru^V. These crystal-field splittings are much larger than those found in Fe^{III} ions, for example.

The effect of long-range magnetic exchange upon the electronic ground state of the resonant atom is equivalent to the existence of a large internal or molecular magnetic field, B_m, which can cause large splittings of the zero-field energy levels (*25, 26*). The magnitude of the splittings is given by $E = mg\beta B_m$, where m is the magnetic quantum number, g is the electronic g-factor, and β is the Bohr magneton. The magnitude of B_m is a function of the ambient temperature, T, and of the ordering temperature, T_N or T_c. From the molecular field theory of a ferromagnetic material it can be shown that

$$B_m(T) = \frac{3kT_c\langle\mu_T\rangle}{J(J+1)g^2\beta^2},$$

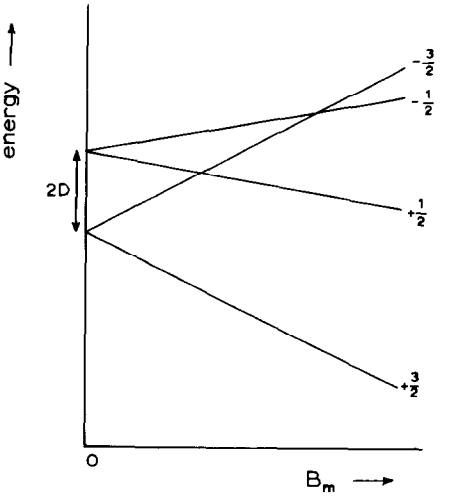

FIG. 10. Schematic representation of the energy level diagram for the $^4A_{2g}$ ground state of Ru^V in the presence of a molecular magnetic field B_m and a crystal-field splitting.

where $\langle \mu_T \rangle$ is the mean magnetic moment in the field direction at temperature T due to the ion with angular momentum J.

If $T_c \simeq 30°K$, $g = 2$, $J = \frac{3}{2}$, and $\langle \mu_0 \rangle \simeq 3.5\beta$, then we find $\beta B_m(0)/k \simeq 20°K$. We shall assume that this represents the order of magnitude to be expected for the molecular field in antiferromagnetic Na_3RuO_4 at $T = 0°K$, and corresponds to an internal magnetic flux density at the nucleus of $B(0) = 58.6$ T. At any temperature between 0 and 30°K, the value of $\beta B_m(T)/k$ can be deduced by scaling in proportion to the value of $B(T)$ in the appropriate Mössbauer spectrum, i.e., $B_m(T)/B_m(0) = B(T)/B(0)$. It is reasonable to assume that the time scale of the exchange interaction is very short compared to the Mössbauer lifetime so that $B_m(T)$ is time independent.

The effect of a molecular magnetic field upon the $^4A_{2g}$ ground state with $2D$ negative is represented in Fig. 10. At $T = 0$ only the lowest state will be populated and a single hyperfine spectrum will be seen. At elevated temperatures the higher levels will become populated. If transitions can take place very rapidly between these levels, then a single averaged field will be recorded by the Mössbauer spectrum. This is normally the case in magnetically concentrated materials where the short interatomic distances for resonant atoms causes relaxation to be fast. If the transitions take place on a slower time scale, comparable with the Mössbauer lifetime for ^{99}Ru (2×10^{-8} sec), then a complex spectrum will be observed.

The lack of an orbital contribution in the $^4A_{2g}$ configuration means that the dominant relaxation mechanism is spin–spin relaxation. Much of the necessary theory has been developed elsewhere in connection with the $^4A_2$ ($S = \frac{3}{2}$) and $^6A_1$ ($S = \frac{5}{2}$) states of the Fe^{III} ion (*27, 28*). The relaxation of the electronic spin S on the resonant atom by a dipole–dipole interaction with all other spins S_j can be represented in the present instance by the truncated Hamiltonian:

$$\mathcal{H} = \left(\frac{\mu_0}{4\pi}\right) g^2\beta^2 \sum_j \frac{1}{r_j^3}(3\cos^2\theta_j - 1)(S_+S_{j-} + S_-S_{j+}),$$

where r_j, θ_j are polar coordinates appropriate to atom j; this is the only term in the full Hamiltonian which involves energy-conserving transitions (*27*). The transition probability for a transition from a state $S_z = m$, $S_{jz} = m'$ to a state $S_z = m'$, $S_{jz} = m$ is given by

$$W(m, m') = \text{constant} \times |\langle m'|\mathcal{H}|m\rangle|^2 \times n(m'),$$

where

$$n(m') = \frac{\exp(-E_{m'}/kT)}{\sum_m \exp(-E_m/kT)}$$

gives the Boltzmann probability that the level at energy $E_{m'}$ is occupied (a necessary condition for relaxation to be possible). Inspection of the matrix element in $W(m, m')$ shows that the transition probabilities are a function of $(1/r_j)^6$, i.e., the relaxation slows down dramatically as the separation r_j between S and S_j increases.

Evaluating the various terms for $W(m, m')$, it is found that the transition probabilities can be expressed in terms of a single time constant C as follows:

m	m'	constant $\times \lvert\langle m'\rvert\mathcal{H}\lvert m\rangle\rvert^2$	$E_{m'}$
$+\frac{3}{2}$	$+\frac{1}{2}$	$9C$	$-2D + 2\beta B_m(T)$
$+\frac{1}{2}$	$+\frac{3}{2}$	$9C$	0
$-\frac{1}{2}$	$-\frac{3}{2}$	$9C$	$6\beta B_m(T)$
$-\frac{3}{2}$	$-\frac{1}{2}$	$9C$	$-2D + 4\beta B_m(T)$
$+\frac{1}{2}$	$-\frac{1}{2}$	$16C$	$-2D + 4\beta B_m(T)$
$-\frac{1}{2}$	$+\frac{1}{2}$	$16C$	$-2D + 2\beta B_m(T)$

The spectrum lineshape can now be calculated using the expressions for $I(p)$ and $G(p)$ used earlier to describe anisotropic relaxation, except that F and W are now 4×4 matrices. We take the diagonal values

of F to be $+1$, $+\frac{1}{3}$, $-\frac{1}{3}$, -1 corresponding to the $S_z = +\frac{3}{2}$, $+\frac{1}{2}$, $-\frac{1}{2}$, $-\frac{3}{2}$ states. The matrix inversion in $G(p)$ is evaluated numerically in complex arithmetic, but results in a large time penalty. Consequently it has not been possible to curve fit this model to the data, and comparison has to be made by visual inspection.

Similar calculations for the $S = \frac{3}{2}$ state of Fe^{III} were aided by the fact that the value of $2D$ could be obtained independently from other data (*27*). In the present instance $2D$ and $B_m(T)$ are unknown, and $B(T)$ is only known accurately when the effects of relaxation on the lineshape are small. Large numbers of spectrum lineshapes were calculated for temperatures of 20, 25, 27 and 28°K, using "reasonable" values of the other parameters. It was found that the value of $\beta B_m(0)/k \simeq 20$°K predicted from the Néel temperature was not unreasonable. Individual computations proved to be remarkably similar to the data, although it was more difficult to find parameters which gave a good simulation of all four spectra. The four curves in Fig. 11 correspond to the parameters $2D = -10$°K, $\beta B_m(0)/k = 20$°K, $C = 5 \times 10^{-9}$ sec, and $B(T) = 53$, 45, 30, and 25 T at 20, 25, 27, and 28°K, respectively, with a linewidth of 0.24 mm sec^{-1}.

At 4.2°K the first excited state is at about 60°K so that relaxation is very slow indeed. At 20°K there is some population of the upper levels, so that although relaxation is still slow there is an additional contribution in the central region of the spectrum. Above 25°K the rapid decrease in the molecular magnetic field causes a rapid increase in the rate of spin–spin relaxation so that motional narrowing occurs.

The predictions from this physically realistic model are encouraging. However, it should be remembered that the simulated spectra in Fig. 11 are calculated on the basis of only *one* internal magnetic field, *one* relaxation time constant, and *one* crystal-field splitting. In Na_3RuO_4 it is quite possible

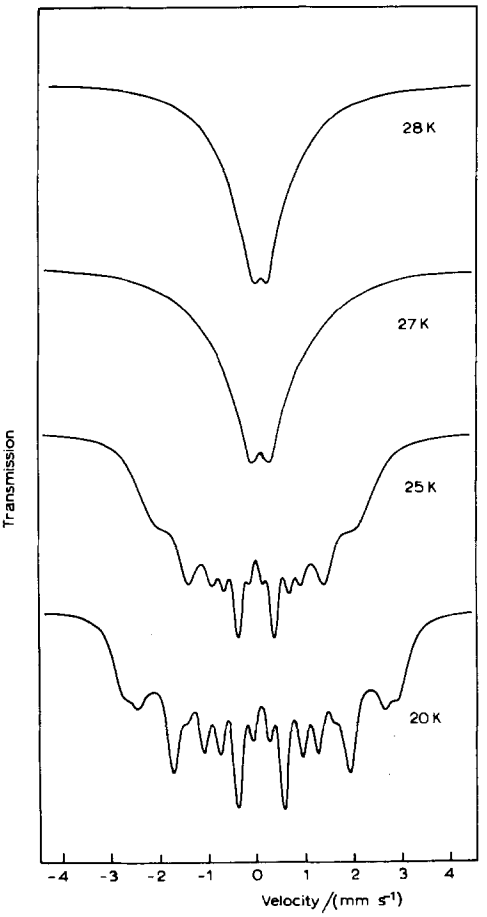

FIG. 11. Simulated spectra using a crystal-field model for slow spin–spin relaxation and antiferromagnetic ordering.

that the two sites do show distinct values of all three parameters. At 20°K a small difference in the internal field (but perhaps much less than that calculated on the basis of a two-field model) would cause line broadening. At 27 and 28°K a small difference in the two relaxation times would cause subtle changes in the conbined lineshape.

It should also be mentioned that it is also possible to use this model to calculate lineshapes for paramagnetic relaxation by setting $B_m(T) = 0$. This gives more accurate results than those illustrated in Fig. 8 but still utilizes incorrect transition probabilities

within the $\pm\frac{1}{2}$ levels because the Hamiltonian is used in truncated form. However, the essential features of Fig. 8 are preserved.

Despite the many assumptions adopted in this crystal-field model of spin–spin relaxation, it is very interesting to see that good agreement with the main features of the data can be obtained for "reasonable" values of the crystal-field splitting and the molecular magnetic field. A more detailed interpretation would require new experimental data with greatly improved resolution and independent determination of the crystal-field splitting.

Conclusions

Na_3RuO_4 has been found to show magnetic hyperfine interactions in the ^{99}Ru spectrum below a temperature of 30°K. The value of the flux density at 4.2°K (58.58 T) is compatible with a saturation field at an $S = \frac{3}{2}$ Ru^V ion, and at intermediate temperatures approximately follows the $S = \frac{3}{2}$ Brillouin function. The concept of tetranuclear intracluster antiferromagnetism is not compatible with the Mössbauer data and is clearly incorrect. It can therefore be concluded that Na_3RuO_4 shows antiferromagnetic three-dimensional long-range order with a Néel temperature of $T_N = 30 \pm 1$°K. From 20 to 30°K the spectra cannot be interpreted on the basis of a single hyperfine field. The assumption of distinct hyperfine fields at the two crystallographic sites appears to be adequate between 20 and 25°K, but cannot explain the data from 25 to 30°K where motional narrowing occurs. The latter is probably due to slow spin–spin relaxation within the crystal-field levels of the $^4A_{2g}$ ground state of the Ru^V ion. Similar relaxation effects have been seen in magnetic systems with considerable anisotropy, such as $KFeCl_3$ and $Fe(N_2H_5)_2(SO_4)_2$ which undergo a transition from three-dimensional to one-dimensional order (*18, 19*). However, it should be noted that there is no evidence for low-dimensional magnetism in Na_3RuO_4, and it seems possible that the unusual structure produces an uncommonly slow spin–spin relaxation. Energy-conserving transitions can only take place between identical atoms, and it may be seen from Fig. 1 that the number of equivalent near-neighbor atoms is small. It is all the more remarkable that this compound is long range ordered, and shows that the magnetic exchange between Ru^V ions is much stronger than had been suspected hitherto. In particular, the intercluster exchange interactions, while probably smaller than the intracluster exchange interactions, are by no means negligible. The behavior in Na_3RuO_4 is clearly different from that found in compounds such as $Ba_3MgRu_2O_9$, where the intracluster exchange across oxygen octahedra sharing a face instead of an edge is clearly much stronger than the intercluster exchange (*29*), although once again long-range order is found at 4.2°K (*30*). Work currently in progress on Sr_2EuRuO_6 shows that long-range interactions can take place via a nominally diamagnetic ($J = 0$) ion along the exchange path Ru^V–O–Eu^{III}–O–Ru^V so that the strength of the intercluster interaction in Na_3RuO_4 may not be as exceptional as it would seem.

Acknowledgments

We are indebted to Dr. J. Darriet of the Laboratoire de Chimie du Solide du CNRS, Université de Bordeaux, France, who supplied us with the sample of Na_3RuO_4 and details of his work prior to publication. We thank the SRC for financial support.

References

1. N. N. GREENWOOD, F. M. DA COSTA, AND R. GREATREX, *Rev. Chim. Minéral.* **13**, 133 (1976).
2. T. C. GIBB, R. GREATREX, N. N. GREENWOOD, AND K. G. SNOWDON, *J. Solid State Chem.* **14**, 193 (1975).
3. J. DARRIET AND A. VIDAL, *C. R. Acad. Sci. Paris Ser. C* **227**, 1235 (1973).

4. J. DARRIET AND J. GALY, *Bull. Soc. Fr. Minéral. Cristallogr.* **97**, 3 (1974).
5. M. DRILLON, J. DARRIET, AND R. GEORGES, *J. Phys. Chem. Solids* **38**, 411 (1977).
6. O. C. KISTNER, *in* "Mössbauer Effect Methodology" (I. J. Gruverman, Ed.), Vol. 3, p. 217, Plenum, New York (1967).
7. T. C. GIBB, R. GREATREX, N. N. GREENWOOD, AND P. KASPI, *J. Chem. Soc. Dalton*, 1253 (1973).
8. N. N. GREENWOOD AND T. C. GIBB, "Mössbauer Spectroscopy," Chapman and Hall, London (1971).
9. A. VAN DEN BERGEN, K. S. MURRAY, B. O. WEST, AND A. N. BUCKLEY, *J. Chem. Soc. A*, 2051 (1969).
10. A. N. BUCKLEY, G. V. H. WILSON, AND K. S. MURRAY, *Solid State Commun.* **7**, 471 (1969).
11. A. N. BUCKLEY, G. V. H. WILSON, AND K. S. MURRAY, *Chem. Commun.*, 718 (1969).
12. A. N. BUCKLEY, I. R. HERBERT, B. D. RUMBOLD, G. V. H. WILSON, AND K. S. MURRAY, *J. Phys. Chem. Solids* **31**, 1423 (1970).
13. B. D. RUMBOLD AND G. V. H. WILSON, *J. Phys. Chem. Solids* **34**, 1887 (1973).
14. M. TAKANO, *J. Phys. Soc. Japan* **33**, 1312 (1972).
15. J. M. D. COEY AND G. A. SAWATZKY, *Phys. Status Solidi B* **44**, 673 (1971).
16. P. K. IYENGAR AND S. C. BHARGAVA, *Phys. Status Solidi B* **46**, 117 (1971).
17. S. C. BHARGAVA AND P. K. IYENGAR, *Phys. Status Solidi B* **53**, 359 (1972); *J. Phys. (Paris) Colloq. C.6* **35**, C6-669 (1974).
18. V. PETROULEAS, A. SIMOPOULOS, AND A. KOSTIKAS, *Phys. Rev. B* **12**, 4675 (1975).
19. C. CHENG, H. WONG, AND W. M. REIFF, *Inorg. Chem.* **16**, 819 (1977).
20. G. K. WERTHEIM, H. J. GUGGENHEIM, H. J. LEVINSTEIN, D. N. E. BUCHANAN, AND R. C. SHERWOOD, *Phys. Rev.* **173**, 614 (1968).
21. M. EIBSCHUTZ, H. J. GUGGENHEIM, AND L. HOLMES, *J. Appl. Phys.* **42**, 1485 (1971).
22. S. DATTAGUPTA AND M. BLUME, *Phys. Rev. B* **10**, 4540 (1974).
23. M. BLUME AND J. A. TJON, *Phys. Rev.* **165**, 446 (1968).
24. KH. S. BAGDASAROV, YU. N. DUBROV, I. N. MAROV, V. O. MARTIROSYAN, AND M. L. MEILMAN, *Phys. Status Solidi B* **56**, K65 (1973).
25. J. CRANGLE, "The Magnetic Properties of Solids," Arnold, London (1977).
26. R. L. CARLIN AND A. J. VAN DUYNEVELDT, "Magnetic Properties of Transition Metal Compounds," Springer-Verlag, New York (1977).
27. H. H. WICKMAN AND C. F. WAGNER, *J. Chem. Phys.* **51**, 435 (1969).
28. M. BLUME, *Phys. Rev. Lett.* **18**, 305 (1967).
29. J. DARRIET, M. DRILLON, G. VILLENEUVE, AND P. HAGENMULLER, *J. Solid State Chem.* **19**, 213 (1976).
30. I. FERNANDEZ, R. GREATREX, AND N. N. GREENWOOD, *J. Solid State Chem.*, in press.